Quantum diffusion and thermalization at resonant tunneling

Carlos A. Parra-Murillo,[1] Javier Madroñero,[2] and Sandro Wimberger[1,3,4]

[1]*Institut für Theoretische Physik, Universität Heidelberg, 69120 Heidelberg, Germany*
[2]*Departamento de Física, Universidad del Valle, Cali, Colombia*
[3]*Dipartimento di Fisica e Scienze della Terra, Università di Parma, Via G. P. Usberti 7/a, 43124 Parma, Italy*
[4]*INFN, Sezione di Milano Bicocca, Gruppo Collegato di Parma, Italy*

Nonequilibrium dynamics and effective thermalization are studied in a resonant tunneling scenario via multilevel Landau-Zener crossings. Our realistic many-body system, composed of two energy bands, naturally allows a separation of degrees of freedom. This gives access to an effective temperature and single- and two-body observables to characterize the delocalization of eigenstates and the nonequilibrium dynamics of our paradigmatic complex quantum system.

PACS number(s): 03.75.Hh, 05.45.Mt, 03.65.Aa, 03.65.Xp

I. INTRODUCTION

Complex systems and their modeling are interesting simply because matter is typically complex. On small scales, quantum mechanics describes interactions and dynamics. One typical example of a complex quantum system are photosynthetic molecules (complexes) in which transport properties seem to be governed by quantum mechanical interference [1]. Strong correlations between the constituents make even "small" systems very complicated. In the helium atom, for instance, classical three-body chaos turns into complicated ionization spectra [2].

The modern experimental tools of atom optics allow for a bottom-up construction of strongly correlated many-body quantum systems [3]. Here we study a lattice model for bosons hitherto hardly investigated [4,5]. Our two-band Bose-Hubbard model shows all the ingredients of a complex quantum system, is realistically implemented with ultracold atoms (see Ref. [6]), and acts as a versatile toolbox to study and control many-body quantum evolutions [6,7]. After introducing the model and a brief review of its spectral properties, we show how thermalization and many-body localization [8–10] in this isolated quantum system depends on its (non)integrability. The latter can be controlled by tunable system parameters; here we use the interparticle interaction strength and a tilt force coupling the two bands. The two bands allow for a natural division into subsystems whose entanglement properties are studied. The purity of the quantum state, which we use to do so, relates to an effective temperature of the subsystems. Finally, we sweep the tilt to investigate the evolution of one- and two-body observables and their thermalization in the course of time.

II. TWO-BAND BOSE-HUBBARD SYSTEM

Our analysis of the spectral (static) and dynamical features is based on the two-band Bose-Hubbard Hamiltonian:

$$\hat{H} = \sum_{l,\beta} \left[-\frac{J_\beta}{2}(\hat{\beta}_{l+1}^\dagger \hat{\beta}_l \, e^{-i2\pi F t} + \text{H.c.}) + \frac{g W_\beta}{2} \hat{\beta}_l^{\dagger 2} \hat{\beta}_l^2 \right]$$
$$+ \sum_{l,\mu} 2\pi F C_\mu \hat{a}_{l+\mu}^\dagger \hat{b}_l \, e^{-i2\mu\pi F t} + \frac{g W_x}{2} \hat{b}_l^{\dagger 2} \hat{a}_l^2 + \text{H.c.}$$
$$+ \sum_l 2g W_x \hat{n}_l^a \hat{n}_l^b + \frac{\Delta}{2}(\hat{n}_l^b - \hat{n}_l^a), \tag{1}$$

where $\hat{\beta}_l(\hat{\beta}_l^\dagger)$ represents the annihilation (creation) operators, and $n_l^\beta = \hat{\beta}_l^\dagger \hat{\beta}_l$ is the number operator, with band index defined as $\beta = \{a,b\}$. $J_{\beta=a,b}$ are the hopping matrix elements, $g W_{a,b,x}$ intra- and interband particle-particle interaction strengths, with $g \in [0,1]$. C_μ represents interband coupling terms induced by the force or, equivalently, by the lattice acceleration F [11,12]. Δ is the band gap, which is controlled by the actual physical implementation [6].

Here we study the behavior of our system in the parameter space (g,F). We impose periodic boundary conditions in space; i.e., $\hat{\beta}_{L+1}^\dagger = \hat{\beta}_1^\dagger$. This allows us to work with the translationally invariant Fock basis (TIFB) defined as in Ref. [13]: $|s_\alpha,\kappa\rangle = D_\alpha^{-1/2} \sum_{k=1}^{D_\alpha} \hat{e}^{-i2\pi\kappa l} \hat{S}^k |\vec{n}_a\rangle_\alpha \otimes |\vec{n}_b\rangle_\alpha$, where $\hat{S} = \hat{S}_a \otimes \hat{S}_b$ is the translation operator of the composite Hilbert space $\mathcal{H}_s = \mathcal{H}_a \otimes \mathcal{H}_b$. The respective dimension is given by $\mathcal{N}_s = (N + 2L - 1)!/LN!(2L-1)!$, for N atoms in L sites. Without loss of generality we work here with the subspace defined by the quasimomentum $\kappa = 0$, resulting in a reduction of the Fock space dimension by a factor of L [6,13].

Our system shows a transition from regular to complex (chaotic) quantum spectra in the vicinity of tunneling resonances [6]. They occur if the tilt compensates exactly the band gap. Resonantly enhanced tunneling (RET) was studied experimentally in the mean-field regime of our model [11] as well as in single-band [12], many-body setups. At RET, i.e., at specific values $F = F_r$ [7], the interband coupling is maximized. r is the order of the resonance, and for simplicity we fix $r = 1$ here. Because of our acceleration gauge, $\hat{H}$ is periodically time-dependent. We naturally use the Floquet approach [14] to study the quasienergies of the system. All energies are measured in recoil energies [3] and the lattice constant is 2π. Then the quasienergies lie in the Floquet zone (FZ), $\varepsilon_i \in [0,2\pi F]$, and the extended spectra are obtained by $\varepsilon_{i,n} = \varepsilon_i + 2\pi n F$, with $n \in \mathbb{Z}$. The numerical implementation is challenging because of the size of the involved Floquet matrices [6].

Figure 1 shows such a spectrum in the (quasi)integrable regime such that the spectral structure can be best appreciated. The regime close to RET is market by δF. In the off-resonant regime, $F \notin [F_r - \delta F/2, F_r + \delta F/2]$, the spectrum can be split into classes of eigenstates, labeled by the upper-band occupation number $M_i = \langle \sum_l \hat{n}_l^b \rangle_{\varepsilon_i}$. The corresponding subsets are referred to as *M manifolds*. While these manifolds
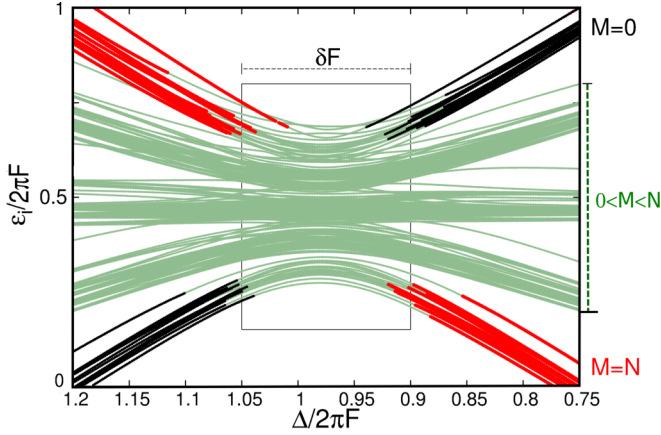
FIG. 1. (Color online) Many-body spectrum around $F_{r=1}$ and $N/L = 4/5$. The different color lines correspond to eigenstates of the type: $|\psi_{M=0}\rangle$ (black lines), $|\psi_{M=N}\rangle$ (red thick lines), and the mixed-like states, i.e., states with $0 < M < N$ are represented by the green thin lines. δF represents the strongly coupled spectral region characterized by avoided crossings. The parameters are chosen for best visibility such that the spectrum is nearly regular. They follow from an implementation with a double-periodic lattice [6]: $\Delta = 1.61$, $J_a = 0.082$, $J_b = -0.13$, $C_0 = -0.094$, $C_{\pm 1} = 0.037$, $C_{\pm 2} = -0.0022$. $W_a = 0.021$, $W_b = 0.026$, and $W_x = 0.023$.

FIG. 2. (Color online) (a) Diffusive spreading of the LDOS at $F_{r=1}$ ($N/L = 6/5$) vs. g. The initial state is: $|\varepsilon_i\rangle \approx \sum_k \hat{S}^k |01110\rangle \otimes |01110\rangle$ at $F = \Delta/3\pi$. (b) standard deviation σ within the manifold $0 < M < N$. (c) IPR in TIFB. The dashed-line is the statistical limit of Ref. [6] [there called random matrix theory (RMT) limit]. (d) Effective temperature computed by means of the purity. M denotes the manifold number defined in text. The parameters are $\Delta = 0.28$, $J_a = 0.038$, $J_b = -0.042$, $C_0 = -0.097$, $C_{\pm 1} = 0.046$, $C_{\pm 2} = -0.0008$, $W_a = 0.028$, $W_b = 0.029$, and $W_x = 0.0286$, for which the spectrum is chaotic around F_r.

substantially increase the complexity of the system with respect to the single-particle or mean-field Landau-Zener tunneling [11], they offer great possibilities to study many-body quantum diffusion [19]. Our two-band model gives a natural separation also into subbands. Their properties and the interband coupling can be investigated by the following two-body correlation functions:

$$\theta_\beta = \left\langle \frac{1}{2} \sum_l \hat{\beta}_l^{\dagger 2} \hat{\beta}_l^2 \right\rangle_{\varepsilon_i}, \quad \text{and} \quad \theta_x = \left\langle 2 \sum_l \hat{n}_l^a \hat{n}_l^b \right\rangle_{\varepsilon_i}, \quad (2)$$

with $\beta = \{a,b\}$. As shown in Ref. [15], the spectrum is well described in the off-resonant regime by the quantum numbers $\{M, \theta_a, \theta_b, \theta_x\}$. This implies a nearly integrable system in this regime, characterized by regular spectral correlations [6,15].

The nonintegrability arises from the increasing degree of manifold mixing at RET. Therein, the loss of good quantum numbers is due to level repulsion, which induce chaotic spectral statistics. In fact, the interplay between interaction (g) and resonant tunneling (F_r) induces a transition from a regular to quantum chaotic spectrum. The conditions for quantum chaos at RET are: $N/L \sim 1$ and $2\pi F r \approx \Delta \leqslant 1$, and $g > 0.5$ (see Ref. [6]).

III. SPECTRAL DIFFUSION

We come now to our main purpose, the study of spectral diffusion and nonequilibrium dynamics. Our system is perfect for this scope, since we can drive an initial state $|\psi_0\rangle$ across the RET regime where nonadiabatic transitions take place. For this, we use a linear sweeping function $F(t) = \dot{F}t + F_0, t \geqslant 0$.

The presence of avoided crossings (ACs) in the spectrum, see Fig. 1, generates a spreading of the wave packet in the instantaneous basis of Floquet states with energies $\varepsilon_i[F(t)]$. For
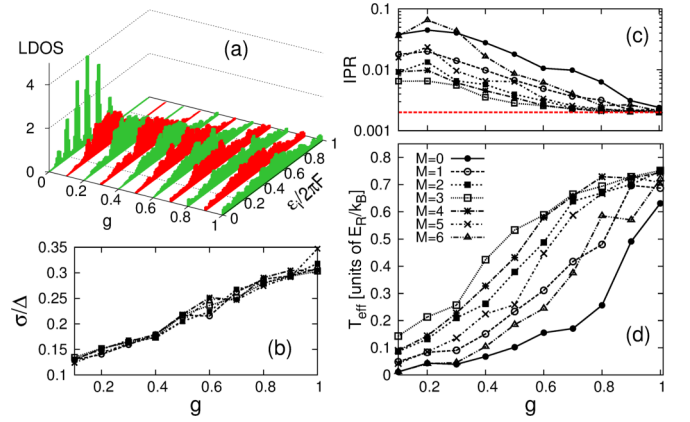
increasing interaction strength g, more and more ACs appear until the spectrum becomes fully chaotic [6]. The local density of states (LDOS), defined by $P_\psi(\varepsilon, g) = \sum_i |C_i|^2 \delta(\varepsilon - \varepsilon_i)$, with $C_i \equiv \langle \psi_t | \varepsilon_i \rangle$, characterizes this spreading [see Fig. 2(a)]. The variance of this probability distribution, see Fig. 2(b), grows almost linearly with g, until a nearly flat distribution is reached within the FZ. Here $|C_i|^2 \sim 1/\mathcal{N}_s$, i.e., the system obeys an equipartition condition. This can be seen also from the Shannon information entropy [16]: $S_{\rm sh} = -\sum_i |C_i|^2 \ln |C_i|^2$, approaching $S_{\rm sh} \approx \ln \mathcal{N}_s$ in statistical equilibrium. We come back to $S_{\rm sh}$ at the end of the paper when studying the reversibility of this equilibration process.

An alternative way to describe the interband mixing is offered by analyzing the subsystems of the total Hilbert space $\mathcal{H}_s = \mathcal{H}_a \otimes \mathcal{H}_b$ provided by the two bands. To do so, we look at the reduced density operator associated with either of the bands after tracing out the other one. The trace is best performed with the help of the following single band states, shifted by k positions in Fock space, $|a(b)_{k,\alpha}\rangle = \hat{S}_{a(b)}^k |\vec{n}_{a(b)}\rangle_\alpha$, since in general $|s_\alpha\rangle \neq |s_\alpha^a\rangle \otimes |s_\alpha^b\rangle$, with $|s_\alpha^{\beta=a,b}\rangle$ being a single-band TIFB state. The density operator of the evolving state, $\hat{\rho}_t = |\psi_t\rangle\langle\psi_t| = \sum_{\alpha,\beta} A_\alpha(t) A_\beta^*(t) |s_\alpha\rangle\langle s_\beta|$, can then be written in this basis as $\hat{\rho}_t = \sum_{kk',\alpha\beta} \Lambda_t^{\alpha\beta} |a_{k,\alpha}\rangle\langle a_{k',\beta}| \otimes |b_{k,\alpha}\rangle\langle b_{k',\beta}|$, with $\Lambda_t^{\alpha\beta} = A_\alpha(t) A_\beta^*(t)(D_\alpha D_\beta)^{-1/2}$. We now trace out the degrees of freedom $\mathcal{H}_b$, which results in

$$\hat{\rho}_t^a = \sum_{k,\alpha} \Lambda_t^{\alpha\alpha} |a_{k,\alpha}\rangle\langle a_{k,\alpha}| = \sum_\alpha \Lambda_t^{\alpha\alpha} \hat{\rho}_{\alpha\alpha}, \quad (3)$$

where we have used $\sum_{p\lambda} \langle b_{p\lambda} | b_{k,\alpha}\rangle\langle b_{k',\beta} | b_{p\lambda}\rangle = \delta_{kk'} \delta_{\alpha\beta}$. The reduced density operator is thus decomposed into a mixture of many-body states $\hat{\rho}_{\alpha\alpha} = \sum_k |a_{k,\alpha}\rangle\langle a_{k,\alpha}|$, with fixed number of particles $0 \leqslant N' \leqslant N$; it is straightforwardly proven that $\text{tr}(\hat{\rho}_t^a) = 1$. The mixedness of ρ_t^a is measured by the purity

$\gamma[\hat{\rho}_t^a] \equiv \text{tr}((\rho_t^a)^2)$, which reads

$$\gamma[\hat{\rho}_t^a] = \gamma[\hat{\rho}_t^b] = \sum_\alpha |A_\alpha(t)|^4. \qquad (4)$$

The result is nothing but the inverse participation ratio, IPR $= \sum_\alpha |A_\alpha(t)|^4$, in the TIFB, a well-known localization measure [17]. Therefore, a well localized state in Fock space has a large purity with an upper bound given by $\gamma = 1$, whenever only one state of TIFB is populated. A fully mixed state has a minimal IPR and its purity is given by the statistical limit $\gamma \approx 2/\mathcal{N}_s$, where the equipartition condition $|A_\alpha|^2 \sim 1/\mathcal{N}_s$ is fulfilled [6].

Tracing over one energy-band, we can characterize the mixedness of the reduced state $\hat{\rho}_t^a$ by an effective temperature T_{eff} for the remaining degrees of freedom. For this, we use a sweep with $\dot{F} = d\delta F$, where d defines the mean level spacing at F_1, we plot the IPR after equilibration, at a time $t \geqslant t_1 = (F_1 - F_0)/\dot{F}$. An effective temperature is then defined by equating the numerically obtained $\gamma[\hat{\rho}_t^a] = \text{IPR}$ with $\gamma[\hat{\rho}_{\text{Th}}(\beta_{\text{eff}})]$, where $\hat{\rho}_t^a \approx Z^{-1} \exp(-\beta_{\text{eff}} \hat{H}_a')$. Here the normalization factor is given by the partition function $Z = Z_\omega \sum_i \exp(-\beta_{\text{eff}} \varepsilon_i')$, with $Z_\omega^{-1} = 1 - \exp(-2\pi F \beta_{\text{eff}})$, taking into account that we are dealing with a Floquet spectrum [18]. $\hat{H}_a'$ is the Hamiltonian for the band a with a number of particles $0 \leqslant N_a \leqslant N$. $\gamma[\hat{\rho}_{\text{Th}}(\beta_{\text{eff}})] = \gamma[\hat{\rho}_t^a] = \text{IPR}$ defines a nonlinear equation for $\beta_{\text{eff}}^{-1} = k_B T_{\text{eff}}$, which is solved by a root finding algorithm.

In Figs. 2(c) and 2(d) we show the IPR and the effective temperature as a function of the interaction strength g. Like in Fig. 2(b), the results are averaged over 30 initial states within each manifold. The number of averaged initial states reduces fluctuations; otherwise, it does not impact the outcome. The more states participate in the evolution, the larger is $\approx \text{IPR}^{-1}$ and hence also T_{eff}. T_{eff} essentially depends only on the manifold number of the initial conditions. For $\langle \psi_0 | \hat{M} | \psi_0 \rangle \approx N/2$, the spreading is faster since the coupling to the neighboring manifolds is more symmetric (see also Fig. 1). Therefore, the respective purity drops faster to $\gamma \approx 2/\mathcal{N}_s$ in this case than for initial states with $\langle \psi_0 | \hat{M} | \psi_0 \rangle \neq N/2$. The latter implies that the temperature is higher the closer one starts to the center of the spectrum at F_0. Our proposal to introduce the effective temperature by the number of effectively coupled states overcomes the problem that a straightforward definition (as usually done in statistical mechanics, e.g., via the entropy) is highly nontrivial in driven systems because of strong fluctuations of the time-dependent quantities; see also the upcoming figures.

The saturation value is obtained from the maximally mixed state reached at $g \approx 1$. For our many-body system, finite-size effects have to be considered. As for the localization measures above, where the dimension $\mathcal{N}_s$ defines a natural lower bound, the effective temperature will saturate to an upper bound depending on the size of the accessible Hilbert space. This explains the behavior of the curves in Fig. 2(d) for $g \to 1$.

IV. EFFECTIVE THERMALIZATION AND IRREVERSIBILITY OF QUANTUM DYNAMICS

The thermalization of observables in a complex quantum system can be investigated on the basis of the eigenstate thermalization hypothesis [8]. First one checks that the
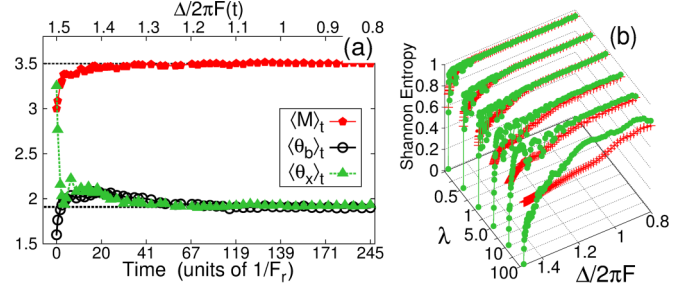

FIG. 3. (Color online) (a) Relaxation and thermalization of single- and two-particle observables for $g = 1$ and $\lambda = 0.25$. In panels (a) and (b) the evolution is defined by the pulse $F(t) = \dot{F}t + F_0$, and $\langle \psi_0 | \hat{M} | \psi_0 \rangle = 3$. (b) Shannon entropy in both instantaneous (greed filled circles) and TIFB basis (red ×) vs. $[\lambda, \Delta/2\pi F(t)]$. The black dashed lines in (a) are the microcanonical averages at $F_{r=1}$ for $N/L = 7/5$. The parameters are the same as described in the legend of Fig. 2.

expectation value of the corresponding operator $\hat{O}$ approaches its diagonal approximation in a finite evolution time, i.e.,

$$\langle \hat{O} \rangle_t \equiv \langle \psi_t | \hat{O} | \psi_t \rangle = \text{tr}(\hat{O} \hat{\rho}_t) \to \sum_i |C_i|^2 O_{ii}, \qquad (5)$$

with $O_{ij} = \langle \varepsilon_i | \hat{O} | \varepsilon_j \rangle$. Second, we test whether the temporal average of an operator characterizing the system is approximately given by

$$\overline{O} = \lim_{t \to \infty} \frac{1}{t} \int_0^t \langle \hat{O} \rangle_{t'} dt' \approx \sum_i |C_i|^2 O_{ii}. \qquad (6)$$

We use the set of observables $\{\hat{M}, \hat{\theta}_{\beta,x}\}$ introduced above to sweep the system from an initial state at $F_0 < F_1$ across the RET regime to a final $F_f > F_1$. Optimal thermalization is then obtained for a sweeping parameter $\lambda \equiv \dot{F}/d\delta F$ of order 1. More specifically, we choose a system with $(N = 7, L = 5)$, giving $\mathcal{N}_s = 2288$, and start at $F_0 = \Delta/3\pi$ with an instantaneous eigenstate $|\varepsilon_i(F_0)\rangle$ within the manifold $M = 3$. We then compute the microcanonical average $O_{\text{mc}} = \Omega_{\delta\varepsilon}^{-1} \sum_i \langle \varepsilon_i(F_1) | \hat{O} | \varepsilon_i(F_1) \rangle$, where $\Omega_{\delta\varepsilon}$ is the number of accessible states within the energy window $\delta\varepsilon = (0.1 - 0.2) 2\pi F$. The results are shown in Fig. 3(a) for our single-particle observable $\hat{M}$ as well as for the two-body correlators $\{\hat{\theta}_{\beta,x}\}$. All their expectation values converge toward their respective microcanonical averages via quantum diffusion across the instantaneous spectrum. For initial states with $M \neq N/2$, these results are confirmed as well, yet the time scale to reach thermalization is then typically larger [cf. also Figs. 2(c) and 2(d)].

The dependence on λ is seen in Fig. 3(b). Full delocalization is only reached for $\lambda \sim 1$ in both energy basis and the TIFB. For $\lambda \gg 1$, the Shannon entropy, as well as the IPR, strongly depend on the chosen basis; hence, the result becomes nonuniversal and depends on the details of the system.

Finally, we present an interesting consequence of the just described diffusion process. Since we sweep the force $F(t)$, the system is no longer autonomous (not even in the Floquet picture) but becomes explicitly (and nonperiodically) time dependent. This makes the sweeping process irreversible in the case of strong (chaotic) thermalization [see Fig. 4(a)].
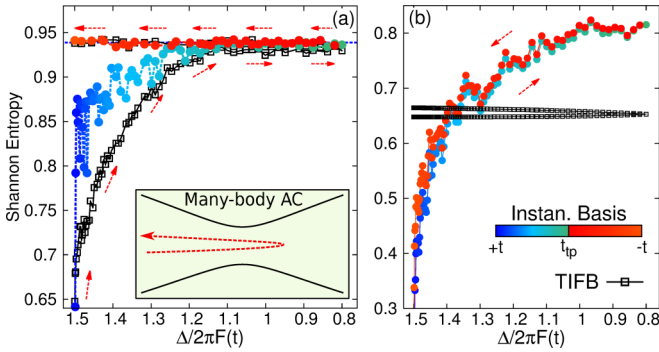
FIG. 4. (Color online) Irreversible (a) and reversible (b) dynamics via sweeping from F_0 to F_f $[F(t) = F_0 + \dot{F}t]$ and back $[F(t) = F_f - \dot{F}t]$, characterized by the Shannon entropy. Entropy in energy basis (color scale: dark-blue/light-red) and entropy in TIFB (black squares). For (a) $\lambda = 1$ and (b) $\lambda = 5 \times 10^3$. The initial state is the same as described in the legend of Fig. 2(a).

However, for fast sweeps with $\lambda \gg 1$, the process is nearly reversible; see Fig. 4(b). Here the system oscillates almost without diffusive spreading between lower and upper band states [e.g., in Fig. 1, it would go from the lower-left to the upper-right states (in black) and back]. The latter is similar to the echoes (revivals) in the fidelity as a function of time, yet here in a full many-body context [20].

V. CONCLUSIONS

In summary, our two-band system is a paradigm example for the implementation (with ultracold atoms) and the study of complex nonequilibrium quantum evolutions. We showed that one may steer the system into equilibrium or keep it relatively coherent (in the sense of quantum reversibility), depending on the specific choice of quench parameters. This paves the way for future experiments on many-body thermalization [9] and new theoretical explorations on optimally controlling the quantum evolution of complex many-body systems [1,21].

[1] G. D. Scholes, T. Mirkovic, D. B. Turner, F. Fassiolia, and A. Buchleitner, Energy Environ. Sci. **5**, 9374 (2012).

[2] G. Tanner, K. Richter, and J.-M. Rost, Rev. Mod. Phys. **72**, 497 (2000); J. S. Parker, B. J. S. Doherty, K. T. Taylor, K. D. Schultz, C. I. Blaga, and L. F. DiMauro, Phys. Rev. Lett. **96**, 133001 (2006); J. Eiglsperger and J. Madroñero, Phys. Rev. A **80**, 022512 (2009).

[3] D. Jaksch and P. Zoller, Ann. Phys. **315**, 52 (2005); I. Bloch, J. Dalibard, and W. Zwerger, Rev. Mod. Phys. **80**, 885 (2008).

[4] V. W. Scarola and S. Das Sarma, Phys. Rev. Lett. **95**, 033003 (2005); J.-P. Martikainen and J. Larson, Phys. Rev. A **86**, 023611 (2012); F. Hebert, Zi Cai, V. G. Rousseau, C. Wu, R. T. Scalettar, and G. G. Batrouni, Phys. Rev. B **87**, 224505 (2013); S. Takayoshi, H. Katsura, N. Watanabe, and H. Aoki, Phys. Rev. A **88**, 063613 (2013).

[5] M. Köhl, H. Moritz, T. Stöferle, K. Günter, and T. Esslinger, Phys. Rev. Lett. **94**, 080403 (2005); T. Müller, Simon Fölling, A. Widera, and I. Bloch, ibid. **99**, 200405 (2007); G. Wirth, M. Ölschläger, and A. Hemmerich, Nat. Phys. **7**, 147 (2010); M. Ölschläger, G. Wirth, T. Kock, and A. Hemmerich, Phys. Rev. Lett. **108**, 075302 (2012).

[6] C. A. Parra-Murillo, J. Madroñero, and S. Wimberger, Phys. Rev. A **88**, 032119 (2013).

[7] P. Plötz, P. Schlagheck, and S. Wimberger, Eur. Phys. J. D **63**, 47 (2011); P. Plötz, J. Madroñero, and S. Wimberger, J. Phys. B **43**, 08001(FTC) (2010).

[8] A. Polkovnikov, K. Sengupta, A. Silva, and M. Vengalattore, Rev. Mod. Phys. **83**, 863 (2011).

[9] T. Kinoshita, T. Wenger, and D. S. Weiss, Nature (London) **440**, 900 (2006); S. Trotzky, Y.-A. Chen, A. Flesch, I. P. McCulloch, U. Schollwöck, J. Eisert, and I. Bloch, Nat. Phys. **8**, 325 (2012); M. Gring, M. Kuhnert, T. Langen, T. Kitagawa, B. Rauer, M. Schreitl, I. Mazets, D. A. Smith, E. Demler, and J. Schmiedmayer, Science **337**, 6100 (2012).

[10] E. Canovi, D. Rossini, R. Fazio, G. E. Santoro, and A. Silva, Phys. Rev. B **83**, 094431 (2011); L. F. Santos, F. Borgonovi, and F. M. Izrailev, Phys. Rev. Lett. **108**, 094102 (2012).

[11] C. Sias, A. Zenesini, H. Lignier, S. Wimberger, D. Ciampini, O. Morsch, and E. Arimondo, Phys. Rev. Lett. **98**, 120403 (2007); A. Zenesini, H. Lignier, G. Tayebirad, J. Radogostowicz, D. Ciampini, R. Mannella, S. Wimberger, O. Morsch, and E. Arimondo, ibid. **103**, 090403 (2009).

[12] J. Simon, S. Bakr, M. Ruichao, M. E. Tai, M. Preiss, and M. Greiner, Nature **472**, 307 (2011); W. S. Bakr, P. M. Preiss, M. E. Tai, R. Ma, J. Simon, and M. Greiner, ibid. **480**, 500 (2011); F. Meinert, M. J. Mark, E. Kirilov, K. Lauber, P. Weinmann, A. J. Daley, and H.-C. Nägerl, Phys. Rev. Lett. **111**, 053003 (2013).

[13] A. R. Kolovsky and A. Buchleitner, Phys. Rev. E **68**, 056213 (2003).

[14] J. H. Shirley, Phys. Rev. **138**, B979 (1965); Y. B. Zeldovich, Sov. Phys. JETP **24**, 1006 (1967).

[15] C. A. Parra-Murillo and S. Wimberger, Acta Phys. Pol. A **124**, 1091 (2013).

[16] R. Blümel and U. Smilansky, Phys. Rev. Lett. **58**, 2531 (1987).

[17] B. Kramer and A. MacKinnon, Rep. Prog. Phys. **56**, 1469 (1993).

[18] R. Ketzmerick and W. Wustmann, Phys. Rev. E **82**, 021114 (2010).

[19] M. Wilkinson, J. Phys. A: Math. Gen. **21**, 4021 (1988); Phys. Rev. A **41**, 4645 (1990).

[20] T. Gorin, T. Prosen, T. H. Seligman, and M. Znidaric, Phys. Rep. **435**, 33 (2006); Ph. Jacquod and C. Petitjean, Adv. Phys. **58**, 67 (2009); P. V. Kuptsov and A. Politi, Phys. Rev. Lett. **107**, 114101 (2011); D. A. Wisniacki and A. J. Roncaglia, Phys. Rev. E **87**, 050902(R) (2013).

[21] F. Platzer, F. Mintert, and A. Buchleitner, Phys. Rev. Lett. **105**, 020501 (2010); R. Heule, C. Bruder, D. Burgarth, and V. M. Stojanović, Phys. Rev. A **82**, 052333 (2010).